ELSEVIER

Forest Ecology and Management 176 (2003) 575–583

Forest Ecology and Management

www.elsevier.com/locate/foreco

Estimating forest biomass using satellite radar: an exploratory study in a temperate Australian *Eucalyptus* forest

Jenet M. Austin, Brendan G. Mackey*, Kimberly P. Van Niel

School of Resources, Environment, and Society, Faculty of Science, The Australian National University, 0200 Canberra, Australia

Received 6 November 2001; accepted 10 June 2002

Abstract

A study was undertaken to explore the relationship between backscattering coefficients from a Japanese Earth Resources Satellite synthetic aperture radar (JERS-1 SAR) image and aboveground biomass sampled at 12 field plots located in Murramarang National Park, New South Wales, Australia. This is the first such investigation in Australian *Eucalyptus* forests. From the field survey we obtained tree and coarse woody debris (CWD) measurements for eight forested, two paddock tree and two grass (effectively zero biomass) plots. Total aboveground and component biomass were estimated for all plots using allometric equations. Live aboveground woody biomass ranged from 0 to 610 t ha^{-1}. The mean JERS-1 SAR backscattering coefficients for the field plot areas ranged from −12.4 to −7.0 dB. The results show positive linear trends between backscattering coefficients and the biomass components of dry *Eucalyptus* forest. The strongest trend was produced with small branch (2 cm) biomass estimates ($r^2 = 0.84$). The biomass saturation level for the JERS-1 SAR data may be higher than estimated by other studies (possibly up to 600 t ha^{-1}), although this trend was not statistically confirmed due to the small sample size ($n = 8$). The results suggest that estimation of forest biomass for biomass inventories in Australia might be possible using satellite radar data when landscape characteristics such as topography, surface water, and forest structure are taken into account.

Keywords: Biomass; SAR; Australia; *Eucalyptus* forest

1. Introduction

Accurate estimation of forest biomass and the division of landcover into CO_2 sources and sinks are required for greenhouse gas inventories, terrestrial carbon accounting, and climate change modelling studies (Dobson et al., 1992). Given the high density of carbon in biomass (about 50%), effective methods are needed for estimating vegetation biomass, particularly in forest ecosystems (Lucas et al., 1998).

Allometric equations are often used to estimate biomass based on empirical relationships between total tree biomass and selected tree attributes. These statistical relationships are derived from a sample of trees taken from a given forested landscape and are dependent on uniformity of tree structure. Allometric equations are commonly derived for each dominant tree species in a forest. Tree biomass is usually correlated

* Corresponding author. Tel.: +61-2-6125-4960; fax: +61-2-6125-3770.
E-mail address: brendan.mackey@anu.edu.au (B.G. Mackey).

0378-1127/02/$ – see front matter
PII: S0378-1127(02)00314-6

with tree height and/or stem diameter. Application of allometric biomass equations therefore requires access to landscape-wide forest inventory data on the specified tree attributes (e.g. height and diameter).

Satellite and airborne remote sensing systems record the surface reflectance of electromagnetic radiation and can generate landscape-wide readily updateable data sets, making them potentially suitable data sources for the estimation of tree parameters over large areas. Radar backscatter is sensitive to the water content of biomass, and data from radar systems can potentially be used to directly estimate aboveground biomass, ultimately producing more accurate maps of carbon stocks, aboveground net primary production and disturbance (Bergen et al., 1998). Consequently, there has been a significant increase in the number of biomass studies using SAR over the last 10 years (Kasischke et al., 1997).

The relationship between SAR backscatter and aboveground biomass has been investigated outside Australia in various forest types, including single species pine forests (Dobson et al., 1992; Kasischke et al., 1995; Pairman et al., 1999), coniferous forests (Le Toan et al., 1992), mixed deciduous and coniferous forests (Ranson and Sun, 1994; Rignot et al., 1994), and tropical forests (Pope et al., 1994; Luckman et al., 1997; Yanasse et al., 1997). Generally, the correlation between forest biomass and SAR backscatter for a single polarisation/wavelength has been found to have a saturation point beyond which the backscatter no longer increases linearly with biomass. The level of saturation has been found to vary as a function of the wavelength and polarisation of the incident radiation (Ranson and Sun, 1997). For example, Ranson and Sun (1994) found that cross-polarised L- and P-band AIRSAR backscatter from coniferous and hardwood boreal forests saturated at approximately 150 t ha^{-1}, while JERS-1 L-band backscatter from rainforest was found to saturate at approximately 100 t ha^{-1} (Spinelli de Araujo et al., 1999).

Despite the availability of radar images for Australia from the Japanese Earth Resources Satellite (JERS-1) since 1992 and airborne data from various sources since 1993 (Lucas et al., 1999), only a few studies have been undertaken using radar backscatter to estimate biomass, vegetation structure, and/or landcover change in Australia, and none of these have been undertaken in Australia's temperate *Eucalyptus* forests. Imhoff et al. (1997) used polarimetric SAR to map vegetation structure for bird habitat studies in Kakadu National Park in the northern Territory, while Milne and Dong (2000) generated a JERS-1 SAR mosaic for vegetation mapping in northern Australia. A major biomass estimation study was conducted in Queensland, Australia (70 field plots) by Lucas et al. (1999) that examined correlations between the biomass of mixed species *Eucalyptus* woodland with SAR backscatter from both airborne and satellite images. The strongest correlation derived from JERS-1 SAR data (L-band, HH polarisation) was with stem biomass ($r^2 = 0.72$, $n = 70$). Lucas et al. (1999) were very positive about the potential for using SAR to estimate biomass in Australian woodlands, which have fewer trees per hectare and consequently have much lower biomass than forested landscapes. The aims of this study were to investigate the relationship between aboveground biomass in an Australian *Eucalyptus* forest and JERS-1 SAR backscatter, and to explore whether saturation occurs at levels similar to those found for other forest types elsewhere in the world. This paper therefore presents the results of the first study on the use of radar for biomass estimation in temperate Australian *Eucalyptus* forests.

2. Site description

The site used for this study was the Murramarang National Park on the south coast of New South Wales (264 km south of Sydney), Australia. The climate of this region is controlled by proximity to the Tasman Sea, with the maritime influence leading to uniformly distributed rainfall throughout the year and an annual average of around 1000 mm. Mean minimum winter temperatures are approximately 6 °C (freezing occurs rarely), while the mean summer maximum is about 24 °C (BOM, 1989, 2000). Murramarang National Park includes both steep and undulating terrain of Permian and Ordovician origins. Vegetation cover ranges structurally from tall closed forest to low woodland, but is predominantly open *Eucalyptus* forest. Patches of rainforest exist in sheltered gullies, representing scattered southern extensions of subtropical forest species (Moore et al., 1991). Common tree species in the forests along the south coast of NSW are *Eucalyptus maculata* (Spotted Gum), *E. pilularis*

(Blackbutt), *E. gummifera* (Red bloodwood), and *E. sieberi* (Silvertop Ash) (Costermans, 1994).

3. Data and methodology

3.1. Field measurements and biomass estimation

In this study, field survey sites were located in the near part (to the satellite) of the SAR image in dry vegetation types on flat terrain. This stratified selection avoided sites that were potentially affected by SAR pixel distortion in the far range, and the confounding impacts of radar backscatter on water, together with the shadowing effects of topography. The eight forested field sites in the study area were selected for homogeneity of vegetation type and structure, and the need to sample a wide range of biomass on relatively flat terrain. Areas burnt or logged between the time of the JERS-1 satellite pass (1993) and the biomass survey (2000) were avoided because these disturbances could result in a lower field estimate of biomass. In addition to the forested field sites, two grass and two paddock tree sites were selected. The grass plots represented sites with effectively zero aboveground biomass, and the two paddock tree sites were selected for their very low aboveground biomass values.

3.2. Field survey

At each of the 12 field sites, the following attributes were measured within a $60 \times 60\ m^2$ plot: diameter at breast height (dbh), height class (5 m intervals) and taxonomy for all trees with a dbh greater than 20 cm; slope angle, slope aspect, and dominant understorey plant species (Table 1). A global positioning system (GPS) was used to locate each plot and the errors did not exceed ± 10 m.

Coarse woody debris (CWD) was measured using the line transect method (van Wagner, 1968) around the perimeters of two $10 \times 10\ m^2$ in opposing plot corners and around a $20 \times 20\ m^2$ in the centre, giving a total transect length of 160 m. Using tallying conditions as described by van Wagner (1968), the diameter, wood origin (*Eucalyptus* or *Acacia*), and decay class (from Chee, 1999) were recorded for each piece of dead wood on the forest floor greater than 5 cm in diameter. All standing dead trees and stumps with a dbh greater than 20 cm were measured for dbh, height and wood type.

3.3. Biomass calculations

Allometric equations from Ash and Helman (1990) were used to calculate tree volumes that were combined with published wood densities (Boland et al., 1992; Bootle, 1983; Costermans, 1994) to produce estimates of small branch, trunk and branch, and whole tree biomass in $t\ ha^{-1}$. These equations were chosen because they were calculated from tree data collected at locations adjacent to Murramarang National Park. Standard error estimates were calculated for the biomass estimates on a plot-by-plot basis to quantify the possible biomass variation within each plot.

CWD volume was calculated using an equation from van Wagner (1968) relating diameter of CWD and transect length to volume of dead wood per unit area. Biomass was then calculated using the wood densities associated with each CWD decay class from Chee (1999). Standing dead biomass (including stumps) was estimated by calculating the volume of each piece of wood from its diameter and height, then multiplying by the wood density of the dominant tree species on the plot.

3.4. JERS-1 SAR image

The SAR image used in this study was from the 23rd of December 1993 (Fig. 1). The JERS-1 SAR system was operated at L-band wavelength (23.5 cm), with horizontal polarisation (transmit and receive), and a look angle of 35°. The SAR data for the study area had mean, maximum, minimum and standard deviation values of −9.079, 6.812, −29.037 and 3.005 dB, respectively (see histogram in Fig. 2).

3.5. Data processing

Some processing of the JERS-1 SAR image had been completed by NASDA (antenna pattern correction, near and far range correction and slant to ground range conversion), producing a pixel size of $18 \times 18\ m^2$. The SAR image was then rectified by manually defining ground control points (GCPs)

Table 1
Characteristics of the 12 plots surveyed, total aboveground biomass = aboveground tree biomass + CWD

Plot ID	Vegetation type	Slope (°)	Aspect (°)	Topographic position	Mean backscattering coefficient (dB) (standard deviation)	Total aboveground biomass, t ha^{-1} (standard error)	Trunk and branch biomass (t ha^{-1}) (standard error)	Small branch biomass (t ha^{-1}) (standard error)	CWD (t ha^{-1}) (standard error)
Pwl	Grass	1	270	Lower slope	−11.5 (2.1)	0 (–)	0 (–)	0 (–)	0
Oval	Grass	0	–	Flat	−11.5 (1.7)	0 (–)	0 (–)	0 (–)	0
PT1	Paddock tree	3	100	Lower slope	−10.9 (2.8)	29.50 (0.22)	25.01 (0.20)	0.001 (0.00)	0
PT2	Paddock tree	2	90	Lower slope	−12.4 (2.5)	42.01 (–)	35.82 (–)	0.001 (–)	1.02
26	*Eucalyptus* forest	2	45	Upper slope	−10.2 (5.5)	87.43 (0.80)	44.61 (0.70)	0.003 (0.00)	35.28
145	*Eucalyptus* forest	3	175	Ridge top	−8.7 (2.2)	217.07 (1.70)	177.96 (1.48)	0.010 (0.00)	9.41
1	*Eucalyptus* forest	7	220	Upper slope	−8.6 (3.0)	324.71 (0.11)	177.80 (0.09)	0.014 (0.00)	112.87
130	*Eucalyptus* forest	4	50	Upper slope	−8.9 (2.2)	370.73 (1.92)	295.49 (1.66)	0.015 (0.00)	28.83
74	*Eucalyptus* forest	9	125	Mid-slope	−8.0 (5.0)	528.00 (2.43)	416.11 (2.16)	0.020 (0.00)	49.61
76	*Eucalyptus* forest	4	25	Ridge top	−7.0 (1.7)	724.95 (3.02)	578.42 (1.44)	0.023 (0.00)	65.72
17	*Eucalyptus* forest	7	115	Ridge top	−8.2 (1.8)	722.69 (2.84)	609.66 (2.57)	0.022 (0.00)	31.54
79	*Eucalyptus* forest	4	60	Upper slope	−7.8 (1.6)	677.17 (5.24)	515.82 (4.67)	0.017 (0.00)	94.92

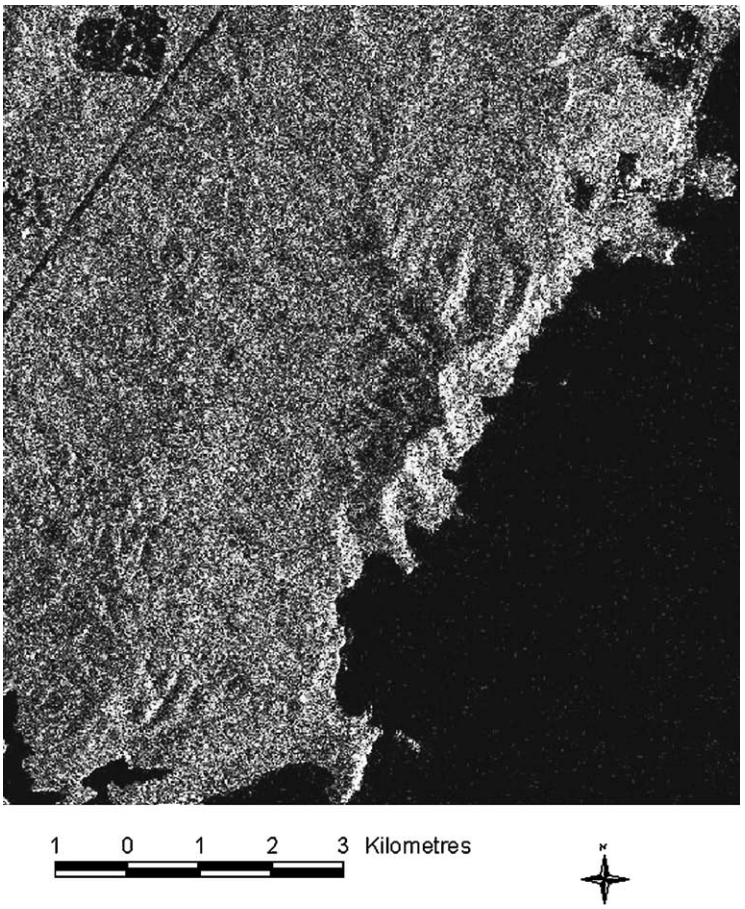

Fig. 1. The portion of the JERS-1 SAR image used in this study (dated 23 December 1993) showing the Murramarang National Park.

within the SAR image. The GCPs were derived from easily distinguishable points in the image (subsequently located using a differential GPS in the field) and from recognisable points in the corresponding optical JERS-1 image for the Murramarang region (previously rectified). Polynomial rectification was used with a linear order. During the rectification process, the pixels were re-sampled using the nearest neighbour technique. The image was rectified to the Australian Geodetic Datum, (AGD) 1966, AMG zone 56.

Radar backscatter is generally used in normalised radar cross-section (NRCS) format (described as the backscattering coefficient and represented by σ^0), for which the standard units are decibels (dB). The SAR image was converted from digital numbers (DNs) to NRCS using the following formula (Spinelli de Araujo et al., 1999):

$$\mathrm{NRCS\,(dB)} = 10\log_{10}(\mathrm{DN}) - 68.5 \quad (1)$$

The locations for all the field plots in this study were co-registered with the rectified SAR image. Speckle reduction was not applied to the entire image because only a small number of the pixels were utilised in this study. Instead, the average backscattering coefficient value in a 3×3 pixel window located over each plot centre was recorded (3×3 pixels corresponded approximately to the size of each field plot). These values were then used to obtain a mean and standard deviation of the backscattering coefficient for the area of each field plot. The 3×3 pixel windows were used in order to reduce the effects of speckle and any rectification errors on the backscattering coefficient values.

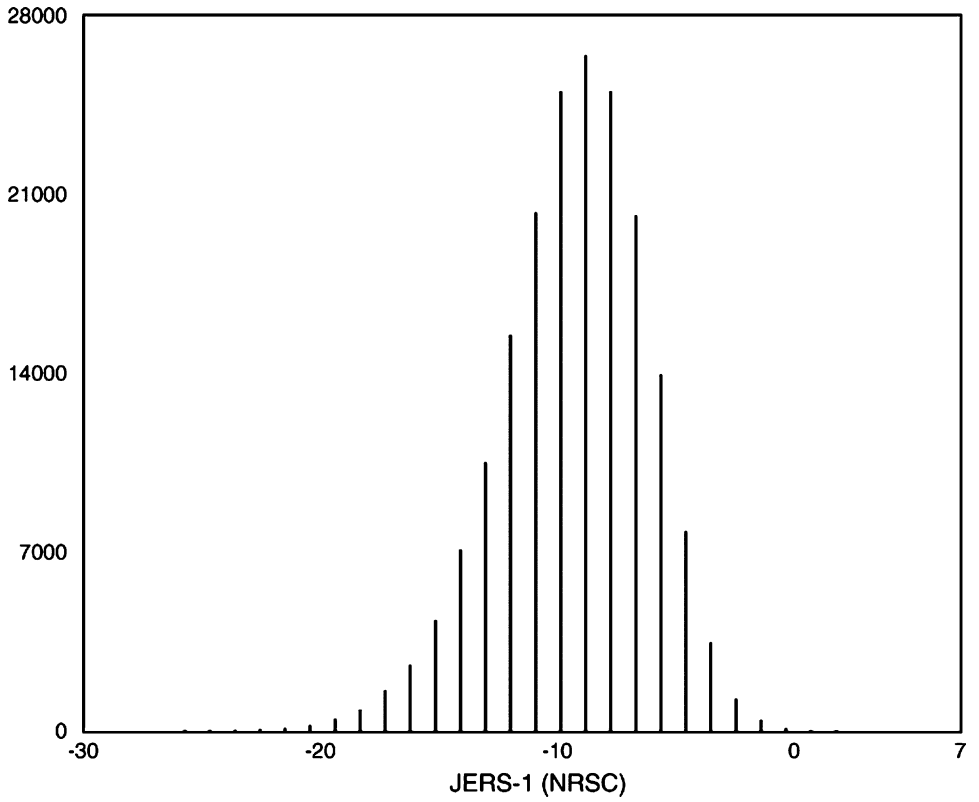

Fig. 2. Histogram showing the range of backscattering coefficient values (dB) for the study area.

3.6. Statistical methods

The small sample size (eight forested plots, four non-forested plots) limited the study to exploratory data analysis (sensu Austin and McKenzie, 1988). Hence the results could only be considered indicative of possible trends. Following the example of a number of similar studies (Harrell et al., 1995; Lucas et al., 1999; Luckman et al., 1997; Ranson and Sun, 1997; Wang et al., 1994), linear regression was used to investigate the relationship between the mean backscattering coefficient and the log of the biomass estimates for the field plots.

3.7. Results and analyses

The mean backscattering coefficients for the field plots ranged from −12.4 to −7.0 dB (Table 1) and were within 2 standard deviations of the mean for the study area. The biomass estimates for the 12 field plots ranged from 0 to 725 t ha^{-1}, and the multiple r^2 values describing the linear relationship between the log of biomass and mean backscattering coefficient ranged from 0.70 (total aboveground biomass) to 0.85 (small branch biomass) (Table 2 and Fig. 3a–d). The results suggest that a trend exists between the backscattering coefficient and the log of the biomass of components of dry *Eucalypt* forest on relatively flat terrain. The highest multiple r^2 value was produced

Table 2
Multiple r^2 values for the linear relationship between L-band backscattering coefficient (dB) and log of biomass (t ha^{-1}), and the residual standard errors for the fit of the regression lines

	Multiple r^2	Residual standard error
Total aboveground biomass	0.7013	1.004
Trunk and branch biomass	0.7117	0.9862
Small branch biomass	0.8465	0.7196
CWD biomass	0.7879	0.8459

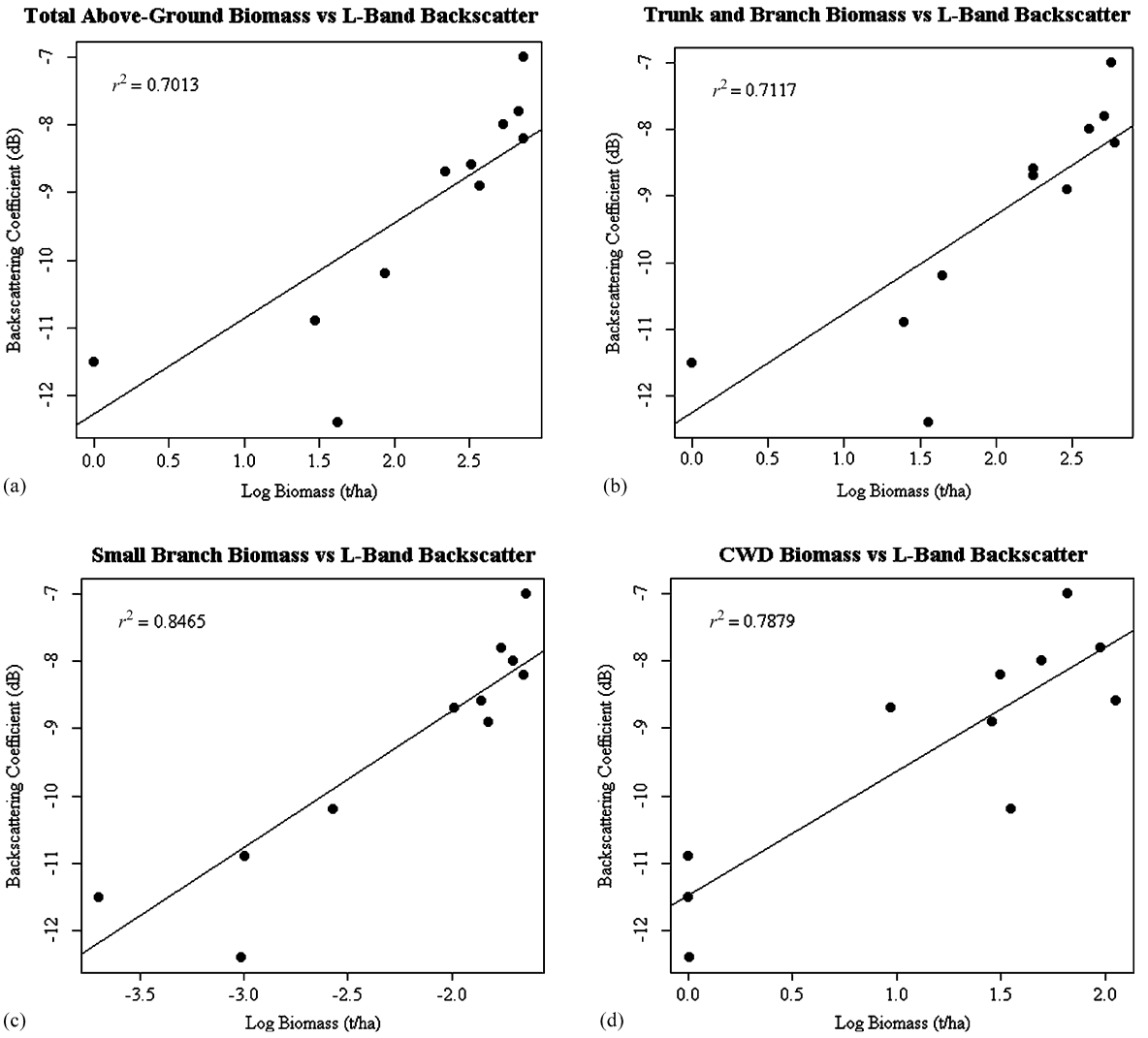

Fig. 3. The log of biomass (t ha^{-1}) versus backscattering coefficient (dB): (a) total aboveground biomass, (b) trunk and branch biomass, (c) small branch (2 cm) biomass, and (d) CWD biomass.

by the small branch component, while the trunk and branch biomass had a slightly higher r^2 value than the total aboveground biomass estimate. CWD also showed a good correlation with an r^2 of 0.79.

4. Discussion and conclusions

4.1. Biomass components

The trunk and branch biomass produced slightly higher r^2 values with mean backscattering coefficient than total aboveground biomass. This was possibly due to the inclusion of leaf and very small branch (<2 cm) biomass in the total aboveground estimate, components unlikely to be detected by the SAR at L-band wavelengths. The relationship between CWD and SAR backscatter was slightly stronger than that of trunk and branch biomass and SAR, which was an interesting result considering that in theory the SAR sensor would not receive backscatter from the CWD because it is dead and would not contain much water. A possible explanation is that the amount of CWD

present on these plots is closely related to the living biomass and therefore produces an r^2 similar to the other biomass components.

The multiple r^2 value for trunk and branch biomass ($r^2 = 0.71$, $n = 8$) obtained in this study is comparable with the results of other studies. A study by Le Toan et al. (1992) on maritime pine in southwestern France using L-band HH airborne SAR data, found a linear correlation with trunk biomass up to 100 t ha^{-1} ($r^2 = 0.73$, $n = 33$). The Australian woodland study by Lucas et al. (1999) obtained an r^2 value of 0.72 ($n = 70$) for the relationship between JERS-1 SAR backscatter and stem biomass up to 100 t ha^{-1} for *Eucalyptus* woodland in Queensland, using very similar techniques to this study. Of interest is that in the present study the r^2 value of 0.71 for trunk and branch biomass (essentially the stem biomass) was obtained using plots with biomass estimates of up to 610 t ha^{-1}.

The small branch (2 cm) biomass produced the strongest correlation with backscatter in this study. This was a surprise considering that other studies have found that the best correlations with L-band SAR backscatter came from stem, branch and total aboveground biomass estimates (for example, Lucas et al., 1999; Milne et al., 1999). However, the above-mentioned studies used allometric equations that calculated leaf biomass rather than small branch biomass and therefore are not directly comparable. The relatively strong correlation obtained in this study was possibly due to the orientation of the 2 cm (diameter) branches in relation to the SAR sensor. It is possible that a sufficient number of 2 cm branches in the forest canopy were positioned so that their orientation coincided with the polarisation of the SAR signal (horizontal for JERS-1 SAR data). If so, a large proportion of the incident radiation could have been scattered directly back to the SAR sensor, thereby accounting for the strong relationship.

4.2. Conclusions

The results suggest that the JERS-1 SAR data could saturate with respect to biomass, at values as high as 600 t ha^{-1} in Australian *Eucalyptus* forest. The small sample size ($n = 12$) restricted the statistical analysis to scatter plot interpretation supported by linear regression. Consequently, the results of this study can be considered as indicative only. However, they do suggest it may be possible to use satellite SAR for the estimation of forest biomass. Further studies using a larger sample size and non-linear regression analysis are necessary to confirm this suggested trend.

Should subsequent studies confirm this trend, additional caveats must be considered before JERS-1 SAR data could be reliably used to predict *Eucalyptus* forest biomass. Our results were based on sites located in a single forest type on relatively flat terrain. Additional biomass field data are therefore required from more complex terrain and from sites with surface water and greater variation in forest structure and species composition. These kinds of additional field data will enable testing of the potential compounding effects of topographic shading, hydrological flows, and vegetation heterogeneity, on the robustness of radar backscatter/biomass relationships. More precise knowledge about weather conditions prevailing during SAR data collection could also improve the biomass/backscatter correlation by helping to account for ephemeral surface water, or by helping to avoid the selection of images from days known to be wet.

Multi-parameter studies, using C-, L- and P-bands data, multiple polarisations, and multiple images could produce stronger correlations between forest biomass and SAR backscatter because the biomass of different *Eucalyptus* forest components may be accounted for separately. Theoretical studies on the structure of *Eucalyptus* forests would advance understanding of the backscattering processes occurring within these forests, possibly accounting for surface interactions not related to biomass, and thereby improving forest biomass/SAR backscatter correlations.

Acknowledgements

The authors would like to thank the School of Resources, Environment, and Society at the Australian National University, NASDA (the Japanese Space Agency and suppliers of the JERS-1 SAR data), and the Japanese National Institute for Environmental Studies. Thanks also go to the ACTION Trust Fund, which awarded a scholarship that helped to fund this study, and we are grateful for comments on data interpretation generously provided by Professor John Richards of the ANU.

References

Ash, J., Helman, C., 1990. Floristics and vegetation biomass of a forest catchment, Kioloa, south coastal New South Wales. Cunninghamia 2 (2), 167–182.

Austin, M.P., McKenzie, N.J., 1988. Data analysis. In: Gunn, R.H., Beattie, J.A., Reid, R.E., van de Graaff, R.H.M. (Eds.), Australian Soil and Land Survey Handbook: Guidelines for Conducting Surveys. Inkata Press, Melbourne, pp. 210–232.

Bergen, K.M., Dobson, M.C., Pierce, L.E., Ulaby, F.T., 1998. Characterising carbon in a northern forest by using SIR-C/X-SAR imagery. Remote Sens. Environ. 63, 24–39.

Boland, D.J., Brooker, M.I.H., Chippendale, G.M., Hall, N., Hyland, B.P.M., Johnson, R.D., Kleinig, D.A., 1992. Forest Trees of Australia. CSIRO, Melbourne.

BOM (Bureau of Meteorology), 1989. Climate Averages Australia, April 1988. Department of Administrative Services, Meteorological Summary, July 1988. Australian Government Publishing Services, Canberra, pp. 357, 360.

BOM (Bureau of Meteorology), 2000. Climate Averages. Bureau of Meteorology, August 17, 2000. http://www.bom.gov.au/climate/averages.

Bootle, K.R., 1983. Wood in Australia: Types, Properties and Use. McGraw-Hill, Sydney.

Chee, Y.E., 1999. A comparison of carbon budgets for a *Pinus radiata* plantation and a native *Eucalypt* forest in Bago State Forest, New South Wales. B.Sc. Geography (Hons.) Thesis. The Australian National University.

Costermans, L., 1994. Native Trees and Shrubs of Southeastern Australia. Lansdowne Publishing, Sydney.

Dobson, M.C., Ulaby, F.T., LeToan, T., Beaudoin, A., Kasischke, E.S., Christensen, N.L., 1992. Dependence of radar backscatter on coniferous forest biomass. IEEE Trans. Geosci. Remote Sens. 30 (2), 412–415.

Harrell, P.A., Bourgeau-Chavez, L.L., Kasischke, E.S., French, N.H.F., Christensen Jr., N.L., 1995. Sensitivity of ERS-1 and JERS-1 radar data to biomass and stand structure in Alaskan boreal forest. Remote Sens. Environ. 54, 247–260.

Imhoff, M.L., Sisk, T.D., Milne, A., Morgan, G., Orr, T., 1997. Remotely sensed indicators of habitat heterogeneity: use of synthetic aperture radar in mapping vegetation structure and bird habitat. Remote Sens. Environ. 60, 217–227.

Kasischke, E.S., Christensen, N.L., Bourgeau-Chavez, L.L., 1995. Correlating radar backscatter with components of biomass in loblolly pine forests. IEEE Trans. Geosci. Remote Sens. 33 (3), 643–659.

Kasischke, E.S., Melack, J.M., Dobson, M.C., 1997. The use of imaging radars for ecological applications—a review. Remote Sens. Environ. 59, 141–156.

Le Toan, T., Beaudoin, A., Riom, J., Guyon, D., 1992. Relating forest biomass to SAR data. IEEE Trans. Geosci. Remote Sens. 30 (2), 403–411.

Lucas, R., Tickle, P., Carter, J., 1998. National Carbon Accounting System Expert Workshop Report: A Proposed Framework for the Inventory and Monitoring of Australia's Forest Biomass. The Australian Greenhouse Office.

Lucas, R.M., Cronin, N., Milne, A.K., Dong, Y., Witte, C., 1999. Estimating woodland biomass stocks in Queensland using synthetic aperture radar (SAR) data. Report to the Australian Bureau of Resource Sciences, Canberra, 54 pp.

Luckman, A., Baker, J., Kuplich, T.M., Yanasse, C.d.C.F., Frery, A.C., 1997. A study of the relationship between radar backscatter and regenerating tropical forest biomass for spaceborne SAR instruments. Remote Sens. Environ. 60, 1–13.

Milne, A.K., Dong, Y., 2000. Vegetation mapping using JERS-1 SAR mosaic for northern Australia. Unpublished Report. School of Geography, University of New South Wales, Sydney, 13 pp.

Milne, A.K., Lucas, R.M., Cronin, N., Dong, Y., Witte, C., 1999. Monitoring biomass using polarimetric multifrequency SAR. Report to the Australian Bureau of Resource Sciences, Canberra.

Moore, D.M., Lees, B.G., Davey, S.M., 1991. A new method for predicting vegetation distributions using decision tree analysis in a geographic information system. Environ. Manage. 15 (1), 59–71.

Pairman, D., McNeill, S., Scott, N., Belliss, S., 1999. Vegetation identification and biomass estimation using AIRSAR data. Geocarto Int. 14 (3), 67–75.

Pope, K.O., Rey-Benayas, J.M., Paris, J.F., 1994. Radar remote sensing of forest and wetland ecosystems in the central American tropics. Remote Sens. Environ. 48, 205–219.

Ranson, K.J., Sun, G., 1994. Mapping biomass of a northern forest using multifrequency SAR data. IEEE Trans. Geosci. Remote Sens. 32 (2), 388–395.

Ranson, K.J., Sun, G., 1997. An evaluation of AIRSAR and SIR-C/X-SAR images for mapping northern forest attributes in Maine, USA. Remote Sens. Environ. 59, 203–222.

Rignot, E., Way, J.B., Williams, C., Viereck, L., 1994. Radar estimates of aboveground biomass in boreal forests of interior Alaska. IEEE Trans. Geosci. Remote Sens. 32 (5), 1117–1124.

Spinelli de Araujo, L.S., dos Santos, J.R., da Costa Freitas, C., Xaud, H.A.M., 1999. The use of microwave and optical data for estimating aerial biomass of the savannah and forest formations at Roraima State, Brazil. In: IEEE 1999 IGARSS Proceedings CD-ROM.

van Wagner, C.E., 1968. The line intersect method in forest fuel sampling. For. Sci. 14 (1), 20–26.

Wang, Y., Kasischke, E.S., Melack, J.M., Davis, F.W., Christensen Jr., N.L., 1994. The effects of changes in loblolly pine biomass and soil moisture on ERS-1 SAR backscatter. Remote Sens. Environ. 49, 25–31.

Yanasse, C.d.C.F., Sant'Anna, S.J.S., Frery, A.C., Renno, C.D., Soares, J.V., Luckman, A.J., 1997. Exploratory study of the relationship between tropical forest regeneration stages and SIR-C L and C data. Remote Sens. Environ. 59, 180–190.